Cancer Research

Dynamic Mast Cell–Stromal Cell Interactions Promote Growth of Pancreatic Cancer

Ying Ma[1], Rosa F. Hwang[2], Craig D. Logsdon[3,4,5], and Stephen E. Ullrich[1,5]

Abstract

Pancreatic ductal adenocarcinoma (PDAC) exists in a complex desmoplastic microenvironment, which includes cancer-associated fibroblasts [also known as pancreatic stellate cells (PSC)] and immune cells that provide a fibrotic niche that impedes successful cancer therapy. We have found that mast cells are essential for PDAC tumorigenesis. Whether mast cells contribute to the growth of PDAC and/or PSCs is unknown. Here, we tested the hypothesis that mast cells contribute to the growth of PSCs and tumor cells, thus contributing to PDAC development. Tumor cells promoted mast cell migration. Both tumor cells and PSCs stimulated mast cell activation. Conversely, mast cell–derived interleukin (IL)-13 and tryptase stimulated PSC proliferation. Treating tumor-bearing mice with agents that block mast cell migration and function depressed PDAC growth. Our findings suggest that mast cells exacerbate the cellular and extracellular dynamics of the tumor microenvironment found in PDAC. Therefore, targeting mast cells may inhibit stromal formation and improve therapy. *Cancer Res; 73(13); 3927–37. ©2013 AACR.*

Introduction

Pancreatic ductal adenocarcinoma (PDAC) is the fourth leading cause of cancer-related death in the United States (1), and from the perspective of cancer mortality it is one of the deadliest diseases (2). With a 5-year relative survival rate of 6% (3), PDAC has an extremely poor prognosis, which is related to its inherent resistance to virtually all therapeutic modalities, including conventional chemotherapy, treatment with targeted agents, radiotherapy, and immunotherapy (3–6).

Tumor cells do not exist in isolation during disease progression. The presence of an intense fibro-inflammatory reaction, composed of immune cells (7) and cancer-associated fibroblasts [also known as the pancreatic stellate cell (PSC); refs. 8, 9], is a prominent pathologic feature of PDAC (10). These components of the microenvironment provide a niche in which pancreatic cancer cells can resist treatment. Essentially, the robust desmoplastic response accompanies the progression from normal histology to a malignant state in human pancreatic cancer (7) and promotes resistance by limiting the delivery of chemotherapeutic agents (5, 9, 11, 12). The cells responsible for the production of the desmoplastic reaction around pancreatic tumors are the PSCs (13).

Several investigators have reported that PSCs promote tumor progression as well as chemoresistance (9, 13–15). PSCs not only increase tumor cell viability *in vitro*, but they also increase tumor invasion and metastasis *in vivo* (9, 14, 15). In addition, PSCs produce secreted factors that render PDAC cells more resistant to therapy (9). Despite these advancements, many unanswered questions remain, particularly those relating to maintenance of the tumor fibrotic microenvironment during disease development.

Ehrlich (as reviewed by Ribatti and Crivellato, ref. 16) was the first to observe mast cell infiltration in chronic inflammation, accompanied by a fibrotic tissue response. Mast cells regulate connective tissue turnover in wound healing, liver cirrhosis, and pulmonary fibrosis (17). Mast cells also regulate adaptive immunity to tumors. Three recent reports indicate that increased numbers of mast cells infiltrating into the PDAC tumor microenvironment represent a poor prognostic indicator (18–20). Mast cell infiltration is zone specific in PDAC, and a high mast cell count in the intratumoral border zone and the distance to the tumor border is an independent risk factor for decreased survival of patients with pancreatic cancer (18). However, it is still unknown whether hindering the migration of mast cells to the tumor site will dampen the aggressiveness of PDAC and/or favor increased survival of tumor-bearing hosts. The dynamic cellular interactions and complex interplay between cell components in the human pancreatic cancer microenvironment have not been well defined. The precise contribution of mast cells remains unknown.

In this study, we investigated the interactions among mast cells, cancer cells, and PSCs. We found that pancreatic cancer cells induce mast cell migration. Treating mast cells with conditioned media from tumor cells and PSCs induced mast

Authors' Affiliations: Departments of [1]Immunology and the Center for Cancer Immunology Research, [2]Surgical Oncology, [3]Cancer Biology, and [4]Gastrointestinal Medical Oncology, The University of Texas MD Anderson Cancer Center; and [5]The University of Texas Graduate School of Biomedical Sciences at Houston, Houston, Texas

Note: Supplementary data for this article are available at Cancer Research Online (http://cancerres.aacrjournals.org/).

Corresponding Author: Stephen E. Ullrich, Department of Immunology, Unit 902, The University of Texas MD Anderson Cancer Center, 1515 Holcombe Boulevard, Houston, TX 77030. Phone: 713-563-3264; Fax: 713-563-3280; E-mail: sullrich@mdanderson.org

doi: 10.1158/0008-5472.CAN-12-4479

cell activation. Conversely, mast cell–derived cytokines interleukin (IL)-13 and tryptase induced increased proliferation of PSCs. IL-13 activated proliferation through the TGF-β2 pathway in a STAT6-independent manner. Blocking mast cell migration and function *in vivo* suppressed PDAC growth and improved survival of PDAC-bearing hosts. Our data suggest that the dynamic cellular and extracellular interactions among mast cells, tumor cells, and stellate cells contribute to the desmoplasia found in pancreatic cancer.

Materials and Methods

Cell culture

Human PDAC, Panc1, BxPC3, and AsPC-1 were obtained from American Type Culture Collection (ATCC). L3.6pl cells were kindly provided by Dr. I.J. Fidler (The University of Texas MD Anderson Cancer Center, Houston, TX). Human PSCs were isolated in primary culture from a surgical specimen of pancreatic adenocarcinoma, and a stable cell line was generated by immortalization (9). The PDAC and PSC cells were cultured in RPMI-1640 (Invitrogen) containing 10% fetal calf serum (FCS) with penicillin and streptomycin (both from Invitrogen) at 37°C in a humidified atmosphere of 5% CO_2. The immortal human pancreatic ductal epithelial cell line (HPDE) was provided as a generous gift from Dr. Ming-Sound Tsao (Ontario Cancer Institute, Toronto, ON, Canada; refs. 21, 22) and was cultured in keratinocyte-serum-free medium (SFM; Invitrogen). The human mast cell lines HMC-1 (kindly provided by Dr. J.H. Butterfield, Mayo Clinic, Rochester, MN), and LAD2 (kindly provided by Dr. A.S. Kirshenbaum, NIH, Bethesda, MD) were cultured as described previously (23, 24). Cell lines were validated by short tandem repeat (STR) DNA fingerprinting by the MD Anderson Cancer Center Characterized Cell Line Core using the AmpFℓSTR Identifiler Kit according to the manufacturer's instructions (Applied Biosystems, cat. no. 4322288). The STR profiles were compared with known ATCC fingerprints (ATCC.org), to the Cell Line Integrated Molecular Authentication database (CLIMA) version 0.1.200808 (http://bioinformatics.istge.it/clima/; Nucleic Acids Research 37: D925-D932 PMCID: PMC2686526), and to the MD Anderson fingerprint database. The STR profiles matched known DNA fingerprints or were unique.

Conditioned media preparation

Human PDAC, PSC, and HPDE cells were grown to 70% to 80% confluence in complete culture media. The medium was changed to serum-free RPMI-1640, and cells were cultured for an additional 48 hours. The nonadherent HMC-1 and LAD2 cells (5×10^5/mL) were resuspended in serum-free RPMI-1640 and cultured for 48 hours. Medium was collected and filtered with 0.22-μm filters (Millipore).

Migration assay

The 8-μm pore Transwell polycarbonate membrane chambers (Corning) were used. A total of 5×10^4 HMC-1 or LAD2 cells in 500 μL SFM was added to the upper chamber. Conditioned media from human PDAC, PSC, or HPDE cells was added into the lower chamber. The cells were allowed to migrate through the membrane for 24 hours at 37°C in 5% CO_2 atmosphere. The nonmigrating cells on the upper surface of the membrane were removed with a cotton swab. The migrating cells in suspension in the lower chamber were fixed in 4% paraformaldehyde. No mast cells were found adherent to the lower surface of the membrane after fixation. Migrating cells were collected, stained with hematoxylin, and counted.

Cell proliferation assay

Proliferation of mast cells, pancreatic cancer cells, and PSCs was assessed using Alamar Blue. Ten microliters of sterile Alamar Blue was added per 5,000 cells. During the incubation period, the conversion of the nonfluorescent indicator dye (resazurin) to a bright red color (resorufin) by metabolically active cells was monitored by reading absorbance at 570 and 600 nm. Proliferation was defined by calculating the percentage conversion of Alamar Blue, as described previously (25).

Mast cell activation and ELISA

Supernatants from cultures of mast cells, mast cells cocultured with PDAC, or mast cells cocultured with PSCs (50:50 mix of cells) were collected, and tryptase secretion was measured by ELISA. Plates were coated with mouse anti-human tryptase antibody (AbD Serotic) and samples were added. Alkaline phosphatase–conjugated mouse anti-human tryptase antibody (Millipore) was used for detection. After adding the substrate, the absorbance was measured at 405 nm. TNF-α release was measured with a Human TNF-α Immunoassay kit (R&D Systems).

Antibody neutralization

PSCs were cultured in mast cell conditioned medium with the following neutralizing antibodies: (i) anti-human tryptase β-2/TPSB2 antibody [monoclonal mouse immunoglobulin G1 (IgG_1) clone #349414; R&D Systems; 4.2 μg/mL equals 3 times the ND50]; and (ii) anti-human IL-13 antibody (monoclonal mouse IgG_1 clone #32116; R&D Systems; 2.2 μg/mL equals 3 times the ND50; ref. 26). Mouse IgG_1 isotype control (monoclonal mouse IgG_1 clone #11711; R&D Systems) was used at the same concentration of the neutralizing antibody. SFM was used as the positive control. Percentage suppression of proliferation = (average proliferation index of antibody blocking group − average proliferation index of negative control group)/(average proliferation index of positive control group − average proliferation index of negative control group) × 100%.

Dye eFluor 670 labeling and flow cytometry analysis

PSCs were labeled with 5 μmol/L eFluor 670 (eBioscience; 10 min at 37°C) and 2×10^4 PSCs were added into each well of a 24-well plate. The cells were then cultured with medium only, mast cell conditioned media, or 2×10^4 HMC-1. Upon 95% confluency (≈8 days), the cells were washed, resuspended in PBS, and supplemented with 2% FBS. Upon cell proliferation, the dye was equally diluted into daughter cells. Fluorescence was measured with a LSRII flow cytometer (BD Biosciences) and analyzed using FlowJo software (Tree Star).

Western blotting

Lysates were prepared from PSCs. Samples containing 40 μg protein per well were loaded in 10% SDS-PAGE and transferred onto polyvinylidene difluoride (PVDF) membranes. Membranes were incubating in blocking buffer (5% nonfat dry milk/PBS) for 1 hour at room temperature, followed by an overnight incubation at 4°C in the presence of antibodies directed against TGF-β2 (R&D Systems), STAT6 (Cell Signaling Technology), pSTAT (Millipore), pSmad2 (Millipore), β-actin (Thermo Scientific), and β-tubulin (Epitomics). Membranes were washed with PBS–0.1% Tween 20 and incubated in the presence of horseradish peroxidase–conjugated secondary antibody. Band detection was carried out by enhanced chemiluminescent substrate (SuperSignal West Dura; Thermo-Fisher Scientific) and captured by X-ray films. Blot quantification was conducted with NIH ImageJ software (http://rsb.info.nih.gov/nih-image/).

Orthotopic implantation of PDAC and AMD3100 or cromolyn treatment

C57BL/6 mice were obtained from The Jackson Laboratory. The mice were maintained in facilities approved by the Association for Assessment and Accreditation of Laboratory Animal Care International in accordance with current regulations and standards of the U.S. Department of Agriculture, Department of Health and Human Services, and NIH. All animal procedures were reviewed and approved by the MD Anderson Cancer Center Animal Care and Use Committee. Orthotopic implantation of PDAC was conducted as described previously (27). Briefly, mice were anesthetized with isoflurane (via inhalation, 4% isoflurane in 96% O_2), and a 1-cm incision in the left subcostal region was made. Murine PDAC cells (Panc-02, or *K-ras*^{G12D}*p53*$^{-/-}$; refs. 5, 28) were injected into the caudal pancreas. The peritoneum and skin were closed with the EZ Clip Wound Closing Kit (Stoelting Co.). Analgesia (buprenorphine; 0.5 mg/kg) was administered postoperatively to minimize pain. Seven days after PDAC implantation, a group of the mice received a CXCR4 chemokine receptor antagonist, AMD3100 (Sigma-Aldrich; 10 μg/mouse, intraperitoneal injection) every Monday, Wednesday, and Friday for 3 weeks, as described previously (27). Another group of the mice received daily injection of cromolyn (10 mg/kg body weight; ref. 29) into the peritoneal cavity. PBS was used as a control. Twenty-eight days after implantation, the mice were sacrificed, and tumor volumes were estimated using the formula ($\pi \times$ long axis $\times$ short axis $\times$ short axis)/6. Mast cell infiltration into the pancreas was measured using Toluidine blue and analyzed using ImageJ software (NIH) as described previously (27). To determine the effect of AMD3100 on survival, drug treatment continued and mice were sacrificed when they became moribund. In those experiments, we implanted C57BL/6 albino mice with *K-ras*^{G12D}*p53*$^{-/-}$ cells transfected with enhanced firefly luciferase (30). At various times after tumor implantation, the mice were injected with D-luciferin (150 μg/mouse; Caliper Life Sciences) and bioluminescence was measured with the IVIS imaging system (Caliper Life Sciences). Tumor volume was measured every week by imaging luciferase signals until the endpoint was reached.

Statistical analysis

Statistical differences between control and experimental groups was determined using the unpaired, two-tailed, Student *t* test; a one-way ANOVA, followed by the Fisher least significant difference (LSD) multiple comparison test; or two-way ANOVA (GraphPad Prism V4 and SPSS for Mac, Inc.). Survival curves were constructed using the Kaplan–Meier method, and statistical significance was determined using the log-rank test. *P* values less than 0.05 were considered statistically significant. Representative experiments are shown; each experiment was repeated independently at least 3 times.

Results

PDAC cells promote mast cell migration

Few mast cells can be found in the normal pancreas; however, it has been reported that increased mast cell numbers in tumor stroma represent a poor prognosis for patients with pancreatic cancer (18–20). Therefore, we first wanted to determine which cell in the tumor microenvironment promoted mast cell migration. We cultured HMC-1 or LAD2 mast cells in conditioned media derived from different pancreatic cancer cells or nontumorigenic PSC or HPDE cells and measured mast cell migration *in vitro*. The 4 pancreatic cancer cells that we used represent different stages of human pancreatic cancer: high (L3.6pl, AsPC-1) or low (Panc-1, BxPC-3) metastatic potential; resistant (Panc-1, AsPC-1) or sensitive (BxPC-3, L3.6pl) to gemcitabine chemotherapy. Compared with the negative control (SFM), conditioned medium from all 4 different pancreatic cancer cell lines significantly upregulated mast cell migration (Fig. 1; $P < 0.0001$). On the other hand, conditioned media from human nontumorigenic pancreatic cell lines did not induce mast cell migration (PSCs vs. SFM, HPDE vs. SFM; $P > 0.05$).

PDAC cells and PSCs stimulate mast cell activation

Next, we determined which elements within the tumor microenvironment affect mast cell function. We asked if coculturing tumor cells or stellate cells with mast cells would result in mast cell activation. Two different human mast cell lines were used, HMC-1 and LAD2. HMC-1 cells represent immature mast cells, do not express the FcεRI receptor, and grow independent of stem cell factor (23). Cytokine (TNF-α) release is a standard method to measure HMC-1 activation (31). LAD2 cells represent mature mast cells with functional FcεRI receptors and are dependent upon stem cell factor for growth (24). More than 98% of LAD2 cells are tryptase-positive, and tryptase released to the culture supernatant is used as a measure of LAD2 activation and degranulation (32). Using these parameters, we tested the ability of human PDAC and PSC cells to activate human mast cells. Compound 48/80 was used as a positive control (33). A significant increase in tryptase release was observed when LAD2 cells were cocultured with all the PDAC cell lines tested ($P < 0.01$ vs. mast cells cultured alone). Similarly, culturing LAD2 with PSCs resulted in a small, but significant tryptase release [Fig. 2A; mast cells (MC) + PSC vs. MC only; $P = 0.001$]. The activation of HMC-1 cells is shown in Fig. 2B. Here again, coculturing the mast cells with the PDAC cell lines or PSCs resulted in a significant increase in TNF-α

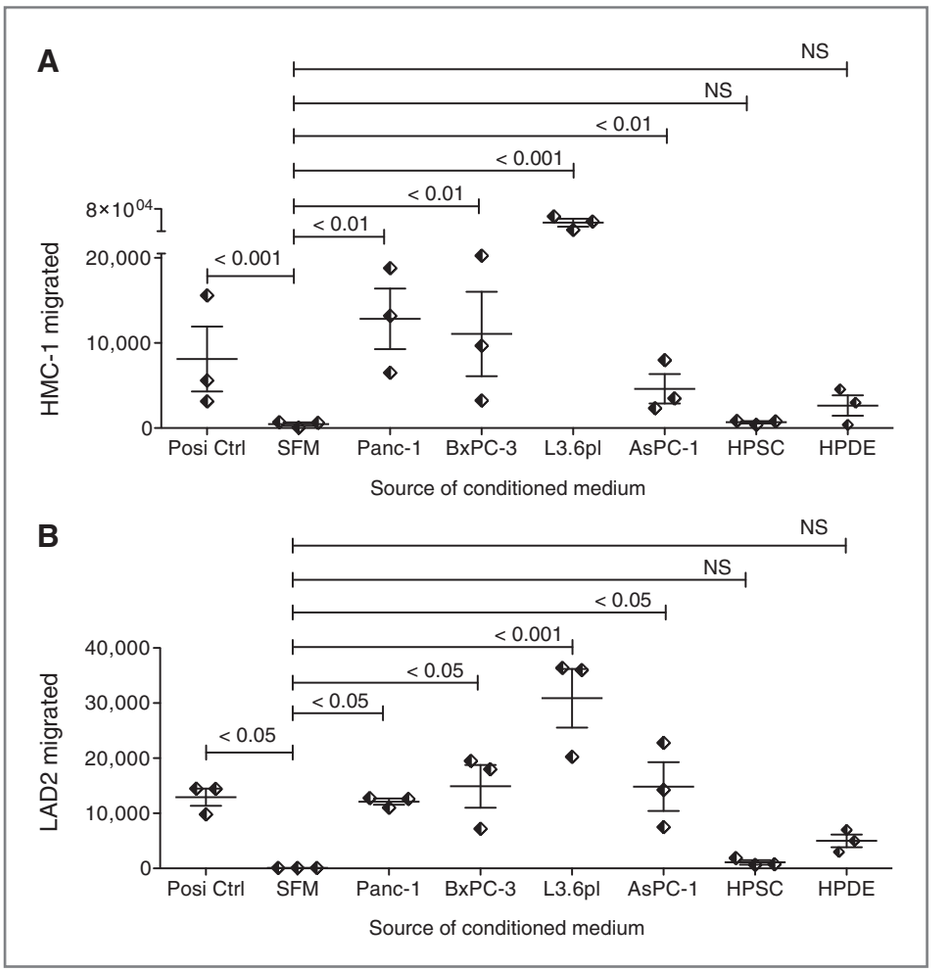

Figure 1. Tumor cells, but neither stellate cells nor ductal epithelial cells, stimulate mast cell migration. HMC-1 (A) and LAD2 (B) mast cells were seeded into the upper chambers of a Transwell chamber, and conditioned media from a variety of PDAC cell lines (Panc-1, BxPC-3, L3.6pl, and AsPC-1) or from nontumorigenic PSCs or HPDE was added to the lower chambers. SFM was used as the negative control; 1% FBS in RPMI-1640 was used as the positive control (Posi Ctrl) for HMC-1, and LAD2 routine culture medium was used as the Posi Ctrl for LAD2. $P < 0.0001$ for all groups was determined by one-way ANOVA, followed by Fisher LSD as the *post hoc* analysis. NS, not statistically significant.

release ($P < 0.001$). Our results indicate that both PDAC and PSC cells trigger mast cell activation.

Conditioned media from mast cells stimulate PDAC proliferation

To investigate the potential role of mast cells in driving tumor growth, we cultured PDAC in mast cell conditioned medium (Fig. 3). Compared with the serum-free controls, mast cell conditioned medium increased proliferation of all 4 of the pancreatic cancer cell lines (Fig. 3A, Panc-1, 13.6% of total increment; Fig. 3B, BxPC-3, 12.4% of total increment; Fig. 3C, L3.6pl, 18.9% of total increment; and Fig 3D, AsPC-1, 16.5% of total increment).

Mast cells promote PSC proliferation

Mast cell influx and fibrosis coexist in chronic inflammation (17), suggesting that there may be a role for mast cells in fibrosis of pancreatic cancer. Therefore, we tested the hypothesis that mast cells affect PSC proliferation. When PSCs were cultured with conditioned medium from mast cells, PSC proliferation increased (Fig. 4A; 14.7% of total increment).

We then measured, by flow cytometry, the doubling times of eFluor 670 dye–labeled PSCs cultured in control medium or mast cell conditioned medium or PSCs cocultured with mast cells. We found that the doubling time of PSCs was decreased when the cells were grown in mast cell conditioned medium (24.15 $\pm$ 0.06 hours), compared with the control (25.04 $\pm$ 0.22 hours; Fig. 4B and C). Strikingly, the doubling time of PSCs cocultured with mast cells was even shorter (22.68 $\pm$ 0.43 hours; Fig. 4B and C). Taken together, these results support our hypothesis that mast cells promote desmoplastic response by inducing PSC proliferation. It seems that both secreted mast cell products and direct cell-to-cell contact are involved; however, direct cell-to-cell contact provides the best stimulus for PSC proliferation.

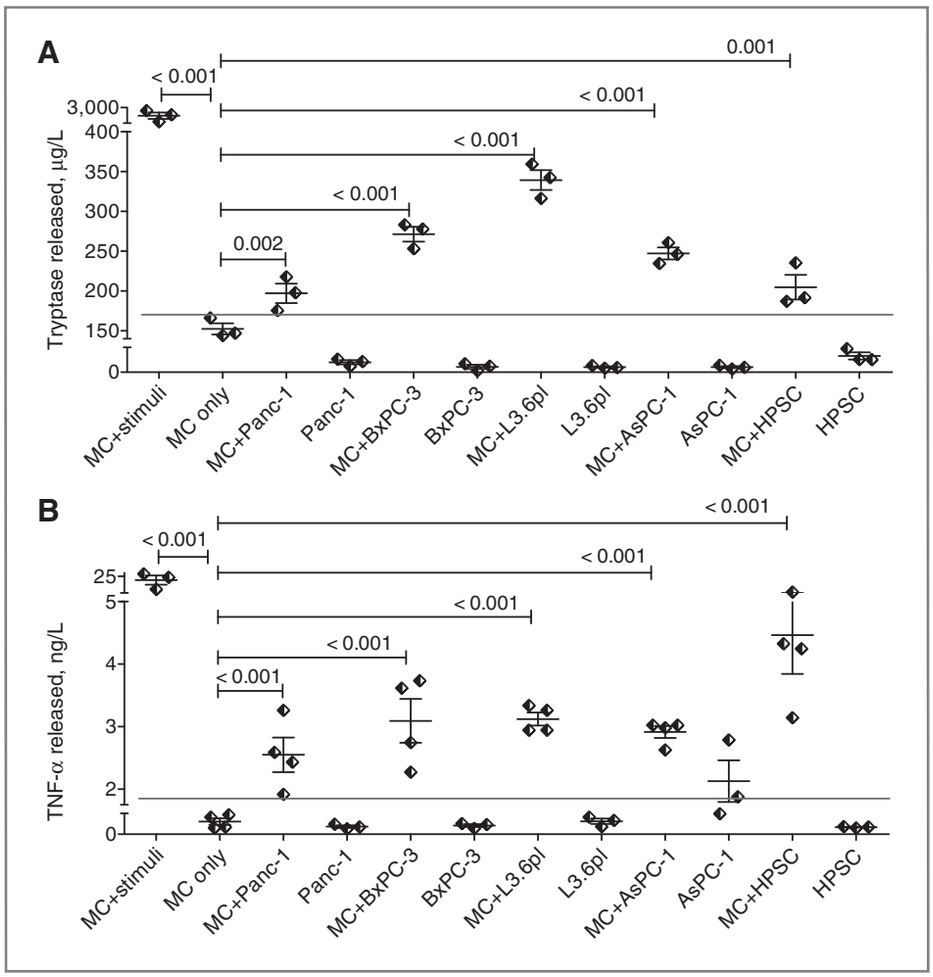

Figure 2. PDAC and PSC cells stimulate mast cell activation. A, LAD2 cells [mast cells (MC)] were cultured with Panc-1, BxPC-3, L3.6pl, and AsPC-1 or the tumor cells were cultured alone for 24 hours; supernatants were collected and tryptase release was determined by ELISA. Similarly, PSCs were cultured alone or with LAD2 cells, and tryptase release was measured (B). HMC-1 cells (MC) were cultured with Panc-1, BxPC-3, L3.6pl, and AsPC-1 or the tumor cells were cultured alone for 24 hours; supernatants were collected, and TNF-α release was determined by ELISA. Similarly, PSCs were cultured alone or with HMC-1 cells, and TNF-α release was measured. As a positive control, mast cells were activated with compound 48/80 (30 μg/mL). $P < 0.0001$ is for all groups as determined by use of a one-way ANOVA, followed by Fisher LSD as the *post hoc* analysis.

Mast cell–derived IL-13 promotes PSC proliferation

IL-13, a mast cell–derived T-helper cell 2 (T_H2)-type cytokine (34), is a major inducer of organ fibrosis. It has been identified as a dominant fibroproliferative cytokine in liver fibrosis induced by schistosomiasis as well as in pulmonary fibrosis caused by asthma via allergic mechanisms (35–37). To determine whether mast cell IL-13 promotes PSC proliferation, we treated mast cell conditioned medium with neutralizing anti-IL-13 antibody. As shown in Fig. 5, neutralizing IL-13 activity suppressed the PSC proliferation (51.53% of blocking rate; $P = 0.0015$), compared with the positive control (IgG1).

We next investigated if the increase in proliferation in PSCs is due to activation of the downstream effectors of IL-13. Stat6 phosphorylation is the latent cytoplasmic event that plays a central role in IL-13–regulated signal transduction and gene expression (38). IL-13 regulation of the TGF-β and phosphor-Smad2 (39) pathway was recently reported to play a role in fibrosis (40, 41). We hypothesized that IL-13 promotes PSC proliferation by regulating Stat6 phosphorylation or TGF-β–pSmad2 pathway. To examine this hypothesis, we evaluated Stat6, phosphorylated Stat6, TGF-β, and pSmad2 expression by Western blotting. Stat6 and phosphorylated Stat6 (Supplementary Fig. S1) expression levels in PSCs were not affected by either mast cell conditioned media or IL-13 antibody blocking. However, TGF-β2, as well as pSmad2, in PSCs (Fig. 5C and D) were upregulated in mast cell conditioned medium, and TGF-β2 expression and Smad2 phosphorylation were modulated by anti-IL-13 antibody. Therefore, we suggest that IL-13 increases PSC proliferation by enhancing TGF-β2 production and Smad2 activation, which is independent of Stat6 or its phosphorylation.

Mast cell–derived tryptase promotes PSC proliferation

Tryptases are serine proteases implicated in asthma and other inflammatory disorders and are highly expressed in human mast cells (42, 43). Tryptase, a potent mitogen for fibroblasts, has been recognized as a molecular link between mast cell activation and fibrosis (44). A recent study showed the importance of tryptase for inducing a cardiac myofibroblastic phenotype, ultimately leading to the development of cardiac fibrosis (45). We hypothesized that tryptase influences PSC proliferation, which is essential to the fibrotic tumor microenvironment. Adding anti-tryptase antibody to mast cell conditioned medium suppressed PSC proliferation (38.06% of blocking rate; $P = 0.0032$; Fig. 5).

Blocking mast cell migration to the tumor microenvironment suppresses PDAC growth and promotes increased survival *in vivo*

Given the fact that PDAC development was suppressed in genetically mast cell–deficient mice (20), we explored pharmacologic approaches to verify that blocking mast cell function can achieve the same effects on PDAC development. CXCR4 is a chemokine receptor that mediates mast cell migration to its ligand, CXCL12 (46). The CXCR4 antagonist (47), AMD3100, blocks mast cell migration *in vivo* (27). To determine if blocking mast cell migration to the tumor microenvironment affects tumor growth *in vivo*, we tested the effect of AMD3100 using an orthotopic model of PDAC. Treating tumor-bearing mice with AMD3100 suppressed tumor volume by 50% [286.6 ± 45.3 mm^3 vs. 574.9 ± 66.2 mm^3 (Fig. 6A; $P < 0.005$; AMD3100 vs. placebo control] and increased survival (Fig. 6B; $P < 0.0142$; AMD3100 vs. placebo control). Decreased tumor size and increased survival were associated with decreased mast cell migration into the tumor site (Fig. 6C–E). Collectively, the data indicate that tumor cells activate mast cell migration to the pancreas, and that blocking mast cell migration *in vivo* suppressed PDAC growth and increased the survival of the tumor-bearing hosts.

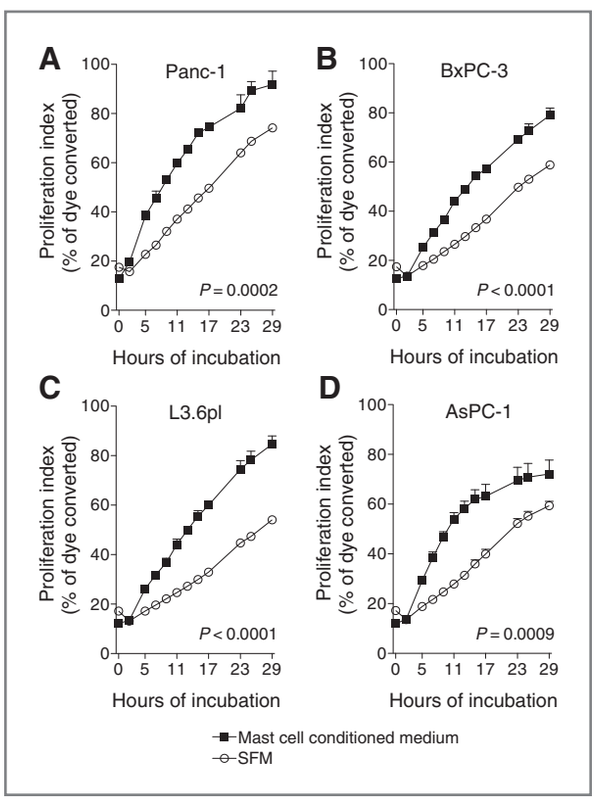

Figure 3. Mast cell conditioned medium promotes cancer cell proliferation. Conditioned medium from mast cells (closed squares) was added to Panc-1 (A), BxPC-3 (B), L3.6pl (C), and AsPC-1 (D). SFM (open circles) was used as the negative control. *P* values were determined using two-way ANOVA.

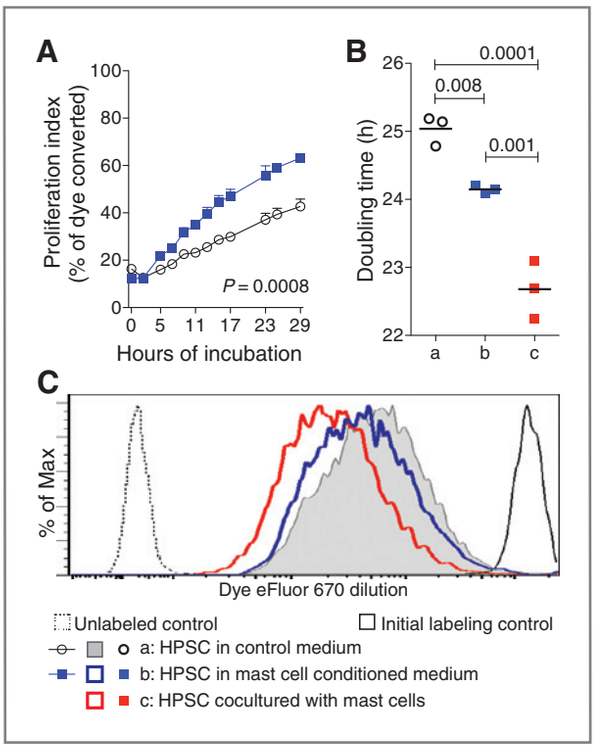

Figure 4. Mast cells accelerate PSC proliferation. A, serum-free mast cell conditioned media (blue squares) increased PSC proliferation. SFM was used as the negative control (black circles). *P* values were determined using two-way ANOVA. B, mast cells decrease PSC cell doubling times. PSCs cultured in medium were used as the control (black circles). Growing PSCs in mast cell conditioned media decreased cell-doubling time (blue squares). Coculturing PSCs with mast cells markedly decreased cell-doubling time (red squares). *P* values from pairwise multiple comparisons were determined using *post hoc* analysis (Fisher LSD). C, PSC proliferation was determined using fluorescent dye dilution. PSC cultured with medium (gray line), mast cell conditioned medium (blue line), or cocultured with mast cells (red line). Initial dye labeling of the PSCs is shown in the black line. Auto-fluorescence of unlabeled cells is shown by the dashed line. The data are representative of at least 5 independent experiments.

Blocking mast cell degranulation results in therapeutic responses to PDAC *in vivo*

To determine whether targeting mast cell function has a therapeutic effect in PDAC, we injected tumor-bearing C57BL/6 mice with cromolyn, a mast cell stabilizer. The growth of surgically implanted *K-ras*^{G12D}*p53*$^{-/-}$ tumors was significantly suppressed by cromolyn treatment (Fig. 7A–E; $P < 0.001$; treated mice vs. saline control at day 42 after treatment). Tumor measurement was conducted at the endtime point (day 50) after treatment. The mean tumor sizes in the saline- and cromolyn-treated groups were 31.3 and 5.2 mm^3, respectively. A *P* value of 0.017 was determined using Student *t* test. Similarly, mast cell degranulation in the tumor microenvironment was inhibited in the cromolyn-treated group compared with the saline-treated control group (Fig. 7A–E). The growth of Panc-02 tumor cells was also significantly suppressed by cromolyn treatment (Supplementary Fig. S2; $P < 0.001$; treated mice vs. saline control

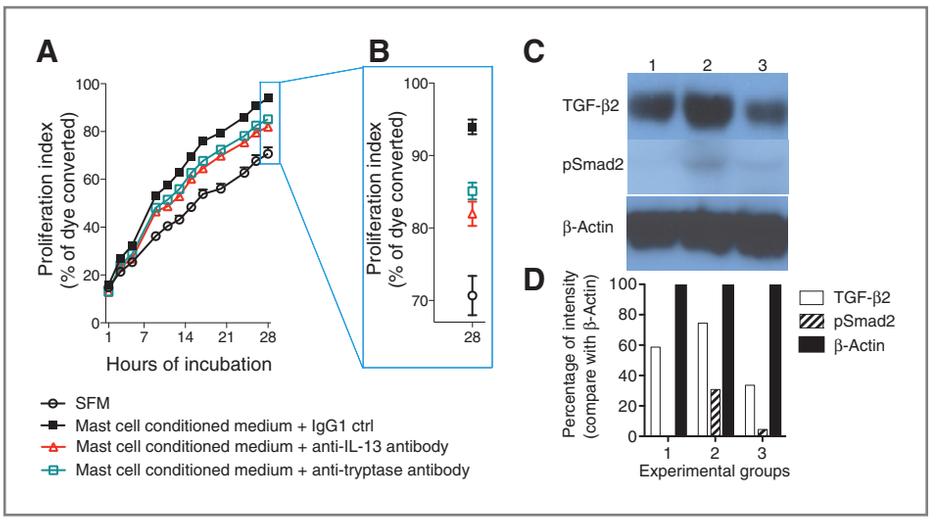

Figure 5. Mast cell–derived IL-13 or tryptase promote stellate cell proliferation. A, serum-free mast cell conditioned medium with anti-human IL-13 antibody (red triangles) blocked PSC proliferation ($P = 0.0015$). Serum-free mast cell conditioned medium with anti-human tryptase antibody (green squares) blocked PSC proliferation ($P = 0.0032$). Serum-free mast cell conditioned medium with IgG1 control antibody (black squares) was used as negative control. SFM was used as the positive control (black circles). *P* values were determined using two-way ANOVA. B, the magnified graph of A at the 28-hour time point. PSC proliferation indexes between groups were presented with mean ± error. Blocking rates for PSC proliferation are 51.53% (anti-IL-13 antibody) and 38.06% (anti-tryptase antibody). C, mast cell–derived IL-13 signaling causes TGF-β2 upregulation and Smad2 phosphorylation. TGF-β2 protein expression and Smad2 phosphorylation were measured in total cell lysates of PSCs by Western blot analysis. Lane 1, PSCs in control medium; lane 2, PSC in mast cell conditioned medium; and lane 3, PSCs in mast cell conditioned medium with blocking IL-13 antibody. D, quantification of TGF-β2 expression and Smad2 phosphorylation was evaluated by ImageJ software. β-Actin was used to normalize the expression density.

at day 21 after treatment). These data further confirm the critical role of mast cells in PDAC progression and suggest that therapies that target mast cell degranulation may be a useful adjuvant treatment of PDAC.

Discussion

PDAC is characterized by a prominent desmoplastic stromal matrix, which promotes tumor growth and blocks the efficient delivery of chemotherapeutic agents (5). In addition, 3 recent

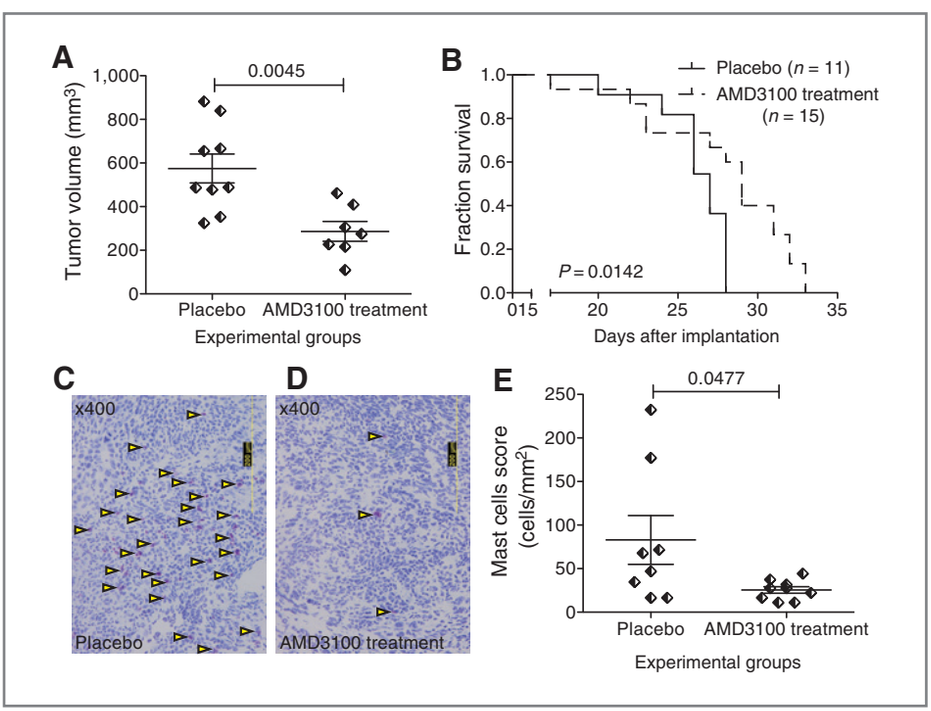

Figure 6. Blocking mast cell migration suppresses PDAC growth. Tumor-bearing C57BL/6 mice treated with the CXCR4 antagonist AMD3100 (10 μg/mouse) and placebo control (saline). A, tumor volume was measured as described. *P* value was determined by Student *t* test. B, AMD3100-treated tumor-bearing mice survived longer than placebo-treated controls. $P = 0.0142$; AMD3100 versus placebo-treated; *P* value was determined by log-rank test. Mast cells migrating to the tumor site (arrows) were identified by Toluidine blue staining placebo-treated control group (C) and the AMD3100-treated group (D). Scale bar, 50 μm. E, quantitative evaluation of mast cell infiltration in pancreatic tissue. *P* value was determined by Student *t* test.

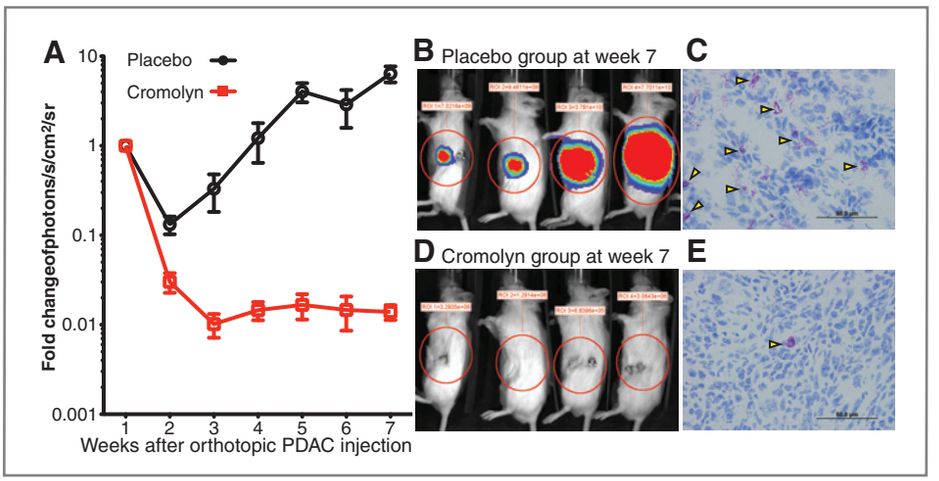

Figure 7. Cromolyn treatment suppresses the growth of PDAC. A, luciferase-transfected *K-ras*^{G12D}*p53*$^{-/-}$ tumor cells were orthotopically implanted into wild-type mice. Seven days later, the mice were injected with cromolyn (10 mg/kg daily). At weekly intervals, the mice were injected with luciferin and the resulting bioluminescence was used to measure tumor size. B, bioluminescent images of mice implanted with luciferase-transfected *K-ras*^{G12D}*p53*$^{-/-}$ tumor cells and injected with saline. C, bioluminescent images of mice implanted with luciferase-transfected *K-ras*^{G12D}*p53*$^{-/-}$ tumor cells and injected with cromolyn. Mast cells (arrowheads) in tumors of saline-treated (D) or cromolyn-treated (E) mice; scale bar, 50 μm.

articles have shown a critical role for mast cells in PDAC (18–20). In this study, we measured the interactions among mast cells, tumor cells, and PSCs to determine how these 3 different elements of the tumor microenvironment contribute to the growth of pancreatic cancer. We found that tumor cells recruit mast cells to the tumor site and stimulate mast cell activation and that blocking mast cell function *in vivo* suppresses tumor growth and increases survival. To our knowledge, this is the first effective example that targeting mast cells in the tumor microenvironment in the immunocompetent PDAC tumor-bearing host can block tumor growth and promote increased survival. Conversely, mast cells stimulate the proliferation of PDAC and PSC cells. We suggest that the cross-talk between mast cells, tumor cells, and stellate cells promotes mast cell migration and activation, promotes cancer growth, and may contribute to the desmoplastic tumor microenvironment that promotes PDAC tumorigenesis.

We found that both the PDAC and PSC cells can trigger mast cell activation and cytokine release. Conversely, mast cell activation favors tumor cell proliferation, suggesting a feedback loop in the tumor microenvironment. Strouch and colleagues (19) reported that mast cells induced the proliferation of 2 gemcitabine-resistant PDAC cell lines (Panc-1 and AsPC-1). Our results confirm this observation and expand the concept to the most representative PDAC cells, including the gemcitabine-sensitive PDAC cell lines (BxPC-3 and L3.6pl). Thus, mast cells stimulate PDAC proliferation regardless of the metastatic potential or drug resistance of the cell line in question.

More importantly, we identified a central role for mast cells in promoting PSC proliferation. Although mast cell conditioned medium stimulated a significant increase in PSC proliferation, the effect was minimal. This may reflect the culture conditions used in this experiment, in which SFM was used. Because we used SFM in the migration experiments shown in Figs. 1 and 2, we wanted to keep the conditions in each experiment as similar as possible. On the other hand, the maximal effect was found when culture conditions allowed for direct contact of mast cells and PSCs. Mixed culture of mast cells and PSCs led to a much shorter doubling time of PSCs than observed when PSCs were treated with mast cell conditioned medium. This may suggest that *in vivo*, direct contact between mast cells and PSCs is required to see the maximal increase in PSC proliferation.

In many different tissues and organs and in a variety of benign and malignant diseases (48), mast cell aggregates are accompanied by fibrosis (49). However, despite the frequent occurrence and severity of the fibrosis, little is known about a cause and effect relationship, and this is particularly true in pancreatic cancer. Our findings indicate that activated mast cells secrete IL-13 and tryptase, which accelerates cancer-associated fibroblast proliferation. This suggests that mast cell infiltration and activation in pancreatic cancer contributes to the dense fibrotic stromal formation that is so prevalent in this disease. With regard to the mechanism of IL-13 in PSC proliferation, we tested a panel of extracellular matrix–related factors, including TGF-β1, TGF-β3, TGF-α, TNF-α, IL-8, stromal cell–derived factor-1 (CXCL12), thymic stromal lymphopoietin (TSLP), fibroblast growth factor 2 (FGF-2), and hyaluronic acid. We found that mast cell–derived IL-13 enhanced TGF-β2 production and Smad2 phosphorylation without regulating Stat6 expression or phosphorylation. This was not totally unexpected, as TGF-β2 has been known to induce extracellular matrix formation (50). This growth-stimulating effect of mast cell–derived IL-13 on stellate cells might lead to the fibrogenesis of pancreatic cancer. None of the other factors mentioned earlier in this report were upregulated by mast cell–derived IL-13 in our study.

Of course, the following must be taken into account in interpreting the data presented here. First, our *in vitro* findings are limited in that only immortalized human tumor cell lines and nontumorigenic cell lines rather than *ex vivo* primary cells were used here. This in part is due to the difficulty in isolating

primary tumor cells. Second, our antibody neutralization studies indicated a role for IL-13 and tryptase in inducing stellate cell proliferation. Antibodies to a whole panel of secreted mast cell products were included in these studies, including TSLP, TSLP receptor, IL-1β, IL-10, and CXCL12; however, only neutralizing tryptase and IL-13 had any effect on PSC proliferation. Also, although we noted a significant reduction in PSC proliferation in the presence of anti-tryptase and/or anti-IL-13, we were not able to reduce PSC proliferation to background levels. This suggests as yet unidentified component(s) in mast cell conditioned medium may be playing a role. Third, although the *in vivo* data presented in Figs. 6 and 7 indicate that both AMD3100 and cromolyn affect mast cell migration into and function in the tumor site, it is important to keep in mind that these agents can affect other cells in the pancreatic tumor microenvironment. Cromolyn has been shown to bind to S100P on pancreatic cancer cells, which prevents the activation of RAGE, thus inhibiting tumor growth and invasion (51). Cromolyn has also been shown to block angiogenesis (52). However, in our analysis, angiogenesis was not affected by cromolyn. We found that cromolyn treatment did not affect the density of CD31-labeled vessels in the tumor microenvironment (data not shown). AMD3100, a CXCR4 antagonist, was used here because it interferes with the *in vivo* migration of mast cells (27). Others have shown, however, that AMD3100 also prevented the noncanonical activation of the sonic hedgehog pathway and the induction of epithelial–mesenchymal transition *in vitro* (53). It is also important to note that both cromolyn and AMD3100 have been shown by others to downregulate the expression of TGF-β (54, 55). On the basis of our observation that mast cell–derived IL-13 upregulation of TGF-β plays a role in the proliferation of stellate cells (Fig. 5), it is entirely possible that both cromolyn and AMD3100 may be playing a similar role here. Regardless of the exact mechanism by which cromolyn and AMD3100 affect pancreatic cancer development, our findings indicate an additional function for these drugs in the tumor microenvironment: inhibition of mast cell migration and function.

In summary, based on our *in vitro* and *in vivo* data, we suggest a new paradigm for how mast cells promote the desmoplastic response that favors PDAC development. Initial mast cell migration was initiated by pancreatic cancer cells, not the stroma or benign cells. Pancreatic cancer cells and stromal cells activated the tumor-infiltrating mast cells as evidenced by degranulation (tryptase release) and cytokine release. Degranulation and secretion of the cytokines from mast cells produced a nourishing microenvironment that triggered a feed-forward loop favoring cancer development. As a result, active mast cells stimulated pancreatic cancer and stromal cell proliferation. The presence of mast cells and their cytokines, including IL-13 and tryptase, in the tumor microenvironment of pancreatic cancer leads to stromal cell proliferation with TGF-β2 production and Smad2 phosphorylation, which eventually culminates in tumor progression. Blocking mast cell migration with the CXCR4-antagonist AMD3100 or inhibiting mast cell degranulation with cromolyn disrupted the feedback loop to a certain extent. This finding may help to explain the significant tumor shrinkage in cromolyn-treated tumor-bearing hosts and longer survival in AMD3100-treated tumor-bearing hosts, which suggests that blocking mast cell function to the tumor microenvironment may be a critical step to interrupt the positive feedback loop of mast cell promoting PDAC progression. The findings reported here provide proof of principal that mast cells contribute to the desmoplastic microenvironment found in PDAC by promoting the proliferation of PSCs. Therefore, treatments targeting mast cell function may be one way to overcome stromal formation and improve PDAC therapy.

Disclosure of Potential Conflicts of Interest

No potential conflicts of interest were disclosed.

Authors' Contributions

Conception and design: Y. Ma, R.F. Hwang, C.D. Logsdon, S.E. Ullrich
Development of methodology: Y. Ma, R.F. Hwang, C.D. Logsdon
Acquisition of data (provided animals, acquired and managed patients, provided facilities, etc.): Y. Ma, S.E. Ullrich
Analysis and interpretation of data (e.g., statistical analysis, biostatistics, computational analysis): Y. Ma, R.F. Hwang, C.D. Logsdon, S.E. Ullrich
Writing, review, and/or revision of the manuscript: Y. Ma, R.F. Hwang, C.D. Logsdon, S.E. Ullrich
Administrative, technical, or material support (i.e., reporting or organizing data, constructing databases): Y. Ma, R.F. Hwang, S.E. Ullrich
Study supervision: C.D. Logsdon, S.E. Ullrich

Acknowledgments

The authors thank Dr. Grzegorz Chodaczek for help with the image analysis, Drs. Patrick Hwu and Weiyi Peng for help with the luciferase labeling experiments, Drs. Chengming Zhu, Omid Tavana, and Zhiqiang Zhang for help with the Western blot analyses, Dr. Stephanie Watowich for critical suggestions, and Nasser Kazimi and Polina Khaskina for help with the animal experiments.

Grant Support

This work was supported by NIH Grant CA131207, Cancer Prevention & Research Institute of Texas Grant RP120777, and by a grant from G.S. Hogan Gastrointestinal Cancer Research Fund (S.E. Ullrich) and a Hirshberg Foundation pancreatic cancer research seed grant (Y. Ma). The Animal Facilities and the Characterized Cell Line Core were supported in part by a National Cancer Institute Core Grant, CA16672.

The costs of publication of this article were defrayed in part by the payment of page charges. This article must therefore be hereby marked *advertisement* in accordance with 18 U.S.C. Section 1734 solely to indicate this fact.

Received December 11, 2012; revised April 11, 2013; accepted April 16, 2013; published OnlineFirst April 30, 2013.

References

1. Jemal A, Siegel R, Xu J, Ward E. Cancer statistics, 2010. CA Cancer J Clin 2010;60:277–300.
2. Fleshman J. Pancreatic cancer: a rare tumor with a devastating health toll. Rare Tumors 2010;2:e52.
3. Chu GC, Kimmelman AC, Hezel AF, DePinho RA. Stromal biology of pancreatic cancer. J Cell Biochem 2007;101:887–907.
4. Neoptolemos JP, Stocken DD, Friess H, Bassi C, Dunn JA, Hickey H, et al. A randomized trial of chemoradiotherapy and chemotherapy after resection of pancreatic cancer. N Engl J Med 2004;350:1200–10.
5. Olive KP, Jacobetz MA, Davidson CJ, Gopinathan A, McIntyre D, Honess D, et al. Inhibition of hedgehog signaling enhances delivery of chemotherapy in a mouse model of pancreatic cancer. Science 2009;324:1457–61.
6. Laheru D, Jaffee EM. Immunotherapy for pancreatic cancer—science driving clinical progress. Nat Rev Cancer 2005;5:459–67.

7. Clark CE, Hingorani SR, Mick R, Combs C, Tuveson DA, Vonderheide RH. Dynamics of the immune reaction to pancreatic cancer from inception to invasion. Cancer Res 2007;67:9518–27.
8. Yen TW, Aardal NP, Bronner MP, Thorning DR, Savard CE, Lee SP, et al. Myofibroblasts are responsible for the desmoplastic reaction surrounding human pancreatic carcinomas. Surgery 2002;131:129–34.
9. Hwang RF, Moore T, Arumugam T, Ramachandran V, Amos KD, Rivera A, et al. Cancer-associated stromal fibroblasts promote pancreatic tumor progression. Cancer Res 2008;68:918–26.
10. Neesse A, Michl P, Frese KK, Feig C, Cook N, Jacobetz MA, et al. Stromal biology and therapy in pancreatic cancer. Gut 2011;60:861–8.
11. Provenzano PP, Cuevas C, Chang AE, Goel VK, Von Hoff DD, Hingorani SR. Enzymatic targeting of the stroma ablates physical barriers to treatment of pancreatic ductal adenocarcinoma. Cancer Cell 2012;21:418–29.
12. Jacobetz MA, Chan DS, Neesse A, Bapiro TE, Cook N, Frese KK, et al. Hyaluronan impairs vascular function and drug delivery in a mouse model of pancreatic cancer. Gut 2013;62:112–20.
13. Apte MV, Park S, Phillips PA, Santucci N, Goldstein D, Kumar RK, et al. Desmoplastic reaction in pancreatic cancer: role of pancreatic stellate cells. Pancreas 2004;29:179–87.
14. Xu Z, Vonlaufen A, Phillips PA, Fiala-Beer E, Zhang X, Yang L, et al. Role of pancreatic stellate cells in pancreatic cancer metastasis. Am J Pathol 2010;177:2585–96.
15. Vonlaufen A, Joshi S, Qu C, Phillips PA, Xu Z, Parker NR, et al. Pancreatic stellate cells: partners in crime with pancreatic cancer cells. Cancer Res 2008;68:2085–93.
16. Ribatti D, Crivellato E. The controversial role of mast cells in tumor growth. Int Rev Cell Mol Biol 2009;275:89–131.
17. Choi KL, Claman HN. Mast cells, fibroblasts, and fibrosis. New clues to the riddle of mast cells. Immunol Res 1987;6:145–52.
18. Cai SW, Yang SZ, Gao J, Pan K, Chen JY, Wang YL, et al. Prognostic significance of mast cell count following curative resection for pancreatic ductal adenocarcinoma. Surgery 2010;149:576–84.
19. Strouch MJ, Cheon EC, Salabat MR, Krantz SB, Gounaris E, Melstrom LG, et al. Crosstalk between mast cells and pancreatic cancer cells contributes to pancreatic tumor progression. Clin Cancer Res 2010;16:2257–65.
20. Chang DZ, Ma Y, Ji B, Wang H, Deng D, Liu Y, et al. Mast cells in tumor microenvironment promotes the *in vivo* growth of pancreatic ductal adenocarcinoma. Clin Cancer Res 2011;17:7015–23.
21. Furukawa T, Duguid WP, Rosenberg L, Viallet J, Galloway DA, Tsao MS. Long-term culture and immortalization of epithelial cells from normal adult human pancreatic ducts transfected by the E6E7 gene of human papilloma virus 16. Am J Pathol 1996;148:1763–70.
22. Ouyang H, Mou L, Luk C, Liu N, Karaskova J, Squire J, et al. Immortal human pancreatic duct epithelial cell lines with near normal genotype and phenotype. Am J Pathol 2000;157:1623–31.
23. Butterfield JH, Weiler DA, Hunt LW, Wynn SR, Roche PC. Purification of tryptase from a human mast cell line. J Leukoc Biol 1990;47:409–19.
24. Kirshenbaum AS, Akin C, Wu Y, Rottem M, Goff JP, Beaven MA, et al. Characterization of novel stem cell factor responsive human mast cell lines LAD 1 and 2 established from a patient with mast cell sarcoma/leukemia; activation following aggregation of FcepsilonRI or FcgammaRI. Leuk Res 2003;27:677–82.
25. Al-Nasiry S, Geusens N, Hanssens M, Luyten C, Pijnenborg R. The use of Alamar Blue assay for quantitative analysis of viability, migration and invasion of choriocarcinoma cells. Hum Reprod 2007;22:1304–9.
26. Kitamura T, Tange T, Terasawa T, Chiba S, Kuwaki T, Miyagawa K, et al. Establishment and characterization of a unique human cell line that proliferates dependently on GM-CSF, IL-3, or erythropoietin. J Cell Physiol 1989;140:323–34.
27. Byrne SN, Limon-Flores AY, Ullrich SE. Mast cell migration from the skin to the draining lymph nodes upon ultraviolet irradiation represents a key step in the induction of immune suppression. J Immunol 2008;180:4648–55.
28. Corbett TH, Roberts BJ, Leopold WR, Peckham JC, Wilkoff LJ, Griswold DP Jr, et al. Induction and chemotherapeutic response of two transplantable ductal adenocarcinomas of the pancreas in C57BL/6 mice. Cancer Res 1984;44:717–26.
29. Soucek L, Lawlor ER, Soto D, Shchors K, Swigart LB, Evan GI. Mast cells are required for angiogenesis and macroscopic expansion of Myc-induced pancreatic islet tumors. Nat Med 2007;13:1211–8.
30. Rabinovich BA, Ye Y, Etto T, Chen JQ, Levitsky HI, Overwijk WW, et al. Visualizing fewer than 10 mouse T cells with an enhanced firefly luciferase in immunocompetent mouse models of cancer. Proc Natl Acad Sci U S A 2008;105:14342–6.
31. Sillaber C, Bevec D, Butterfield JH, Heppner C, Valenta R, Scheiner O, et al. Tumor necrosis factor alpha and interleukin-1 beta mRNA expression in HMC-1 cells: differential regulation of gene product expression by recombinant interleukin-4. Exp Hematol 1993;21:1271–5.
32. Guhl S, Babina M, Neou A, Zuberbier T, Artuc M. Mast cell lines HMC-1 and LAD2 in comparison with mature human skin mast cells—drastically reduced levels of tryptase and chymase in mast cell lines. Exp Dermatol 2010;19:845–7.
33. Koibuchi Y, Ichikawa A, Nakagawa M, Tomita K. Histamine release induced from mast cells by active components of compound 48/80. Eur J Pharmacol 1985;115:163–70.
34. Klein M, Klein-Hessling S, Palmetshofer A, Serfling E, Tertilt C, Bopp T, et al. Specific and redundant roles for NFAT transcription factors in the expression of mast cell-derived cytokines. J Immunol 2006;177:6667–74.
35. Wynn TA. Fibrotic disease and the T(H)1/T(H)2 paradigm. Nat Rev Immunol 2004;4:583–94.
36. Chiaramonte MG, Donaldson DD, Cheever AW, Wynn TA. An IL-13 inhibitor blocks the development of hepatic fibrosis during a T-helper type 2-dominated inflammatory response. J Clin Invest 1999;104:777–85.
37. Lee CG, Homer RJ, Zhu Z, Lanone S, Wang X, Koteliansky V, et al. Interleukin-13 induces tissue fibrosis by selectively stimulating and activating transforming growth factor beta(1). J Exp Med 2001;194:809–21.
38. Kelly-Welch AE, Hanson EM, Boothby MR, Keegan AD. Interleukin-4 and interleukin-13 signaling connections maps. Science 2003;300:1527–8.
39. Laping NJ, Everitt JI, Frazier KS, Burgert M, Portis MJ, Cadacio C, et al. Tumor-specific efficacy of transforming growth factor-beta RI inhibition in Eker rats. Clin Cancer Res 2007;13:3087–99.
40. Shinozaki S, Mashima H, Ohnishi H, Sugano K. IL-13 promotes the proliferation of rat pancreatic stellate cells through the suppression of NF-kappaB/TGF-beta1 pathway. Biochem Biophys Res Commun 2010;393:61–5.
41. Fichtner-Feigl S, Strober W, Kawakami K, Puri RK, Kitani A. IL-13 signaling through the IL-13alpha2 receptor is involved in induction of TGF-beta1 production and fibrosis. Nat Med 2006;12:99–106.
42. Miller JS, Moxley G, Schwartz LB. Cloning and characterization of a second complementary DNA for human tryptase. J Clin Invest 1990;86:864–70.
43. Vanderslice P, Ballinger SM, Tam EK, Goldstein SM, Craik CS, Caughey GH. Human mast cell tryptase: multiple cDNAs and genes reveal a multigene serine protease family. Proc Natl Acad Sci U S A 1990;87:3811–5.
44. Ruoss SJ, Hartmann T, Caughey GH. Mast cell tryptase is a mitogen for cultured fibroblasts. J Clin Invest 1991;88:493–9.
45. McLarty JL, Melendez GC, Brower GL, Janicki JS, Levick SP. Tryptase/protease-activated receptor 2 interactions induce selective mitogen-activated protein kinase signaling and collagen synthesis by cardiac fibroblasts. Hypertension 2011;58:264–70.
46. Juremalm M, Hjertson M, Olsson N, Harvima I, Nilsson K, Nilsson G. The chemokine receptor CXCR4 is expressed within the mast cell lineage and its ligand stromal cell-derived factor-1alpha acts as a mast cell chemotaxin. Eur J Immunol 2000;30:3614–22.
47. Hatse S, Princen K, Bridger G, De Clercq E, Schols D. Chemokine receptor inhibition by AMD3100 is strictly confined to CXCR4. FEBS Lett 2002;527:255–62.
48. Ahmed A, Powers MP, Youker KA, Rice L, Ewton A, Dunphy CH, et al. Mast cell burden and reticulin fibrosis in the myeloproliferative neoplasms: a computer-assisted image analysis study. Pathol Res Pract 2009;205:634–8.

49. Chiu A, Nanaji NM, Czader M, Gheorghe G, Knowles DM, Chadburn A, et al. The stromal composition of mast cell aggregates in systemic mastocytosis. Mod Pathol 2009;22:857–65.

50. Saika S, Saika S, Liu CY, Azhar M, Sanford LP, Doetschman T, et al. TGFbeta2 in corneal morphogenesis during mouse embryonic development. Dev Biol 2001;240:419–32.

51. Arumugam T, Ramachandran V, Logsdon CD. Effect of cromolyn on S100P interactions with RAGE and pancreatic cancer growth and invasion in mouse models. J Natl Cancer Inst 2006;98:1806–18.

52. Theoharides TC. Mast cells and pancreatic cancer. N Engl J Med 2008;358:1860–1.

53. Li X, Ma Q, Xu Q, Liu H, Lei J, Duan W, et al. SDF-1/CXCR4 signaling induces pancreatic cancer cell invasion and epithelial–mesenchymal transition *in vitro* through non-canonical activation of Hedgehog pathway. Cancer Lett 2012;322:169–76.

54. Palaniyandi Selvaraj S, Watanabe K, Ma M, Tachikawa H, Kodama M, Aizawa Y. Involvement of mast cells in the development of fibrosis in rats with postmyocarditis dilated cardiomyopathy. Biol Pharm Bull 2005;28:2128–32.

55. Kim JH, Kolozsvary A, Jenrow KA, Brown SL. Plerixafor, a CXCR4 antagonist, mitigates skin radiation-induced injury in mice. Radiat Res 2012;178:202–6.